RESEARCH ARTICLE

PROTEINS WILEY

Molecular investigation of the tandem Tudor domain and plant homeodomain histone binding domains of the epigenetic regulator UHRF2

Shane M. Ginnard[1] | Alyssa E. Winkler[1] | Carlos Mellado Fritz[1] | Tatum Bluhm[1] | Ray Kemmer[1] | Marisa Gilliam[1] | Nick Butkevich[1] | Sara Abdrabbo[1] | Kaitlyn Bricker[1] | Justin Feiler[1] | Isaak Miller[1] | Jenna Zoerman[1] | Zeineb El-Mohri[1] | Panida Khuansanguan[1] | Madyson Basch[1] | Timothy Petzold[1] | Matthew Kostoff[1] | Sean Konopka[1] | Brendon Kociba[1] | Thomas Gillis[1] | Deborah L. Heyl[1] | Raymond C. Trievel[2] | Brittany N. Albaugh[1] 🆔

[1]Department of Chemistry, Eastern Michigan University, Ypsilanti, Michigan, USA

[2]Department of Biological Chemistry, University of Michigan, Ann Arbor, Michigan, USA

Correspondence
Brittany N. Albaugh, Department of Chemistry, Eastern Michigan University, Ypsilanti, MI 48197, USA.
Email: balbaug1@emich.edu

Abstract

Ubiquitin-like containing PHD and ring finger (UHRF)1 and UHRF2 are multidomain epigenetic proteins that play a critical role in bridging crosstalk between histone modifications and DNA methylation. Both proteins contain two histone reader domains, called tandem Tudor domain (TTD) and plant homeodomain (PHD), which read the modification status on histone H3 to regulate DNA methylation and gene expression. To shed light on the mechanism of histone binding by UHRF2, we have undergone a detailed molecular investigation with the TTD, PHD and TTD-PHD domains and compared the binding activity to its UHRF1 counterpart. We found that unlike UHRF1 where the PHD is the primary binding contributor, the TTD of UHRF2 has modestly higher affinity toward the H3 tail, while the PHD has a weaker binding interaction. We also demonstrated that like UHRF1, the aromatic amino acids within the TTD are important for binding to H3K9me3 and a conserved aspartic acid within the PHD forms an ionic interaction with R2 of H3. However, while the aromatic amino acids in the TTD of UHRF1 contribute to selectivity, the analogous residues in UHRF2 contribute to both selectivity and affinity. We also discovered that the PHD of UHRF2 contains a distinct asparagine in the H3R2 binding pocket that lowers the binding affinity of the PHD by reducing a potential electrostatic interaction with the H3 tail. Furthermore, we demonstrate the PHD and TTD of UHRF2 cooperate to interact with the H3 tail and that dual domain engagement with the H3 tail relies on specific amino acids. Lastly, our data indicate that the unique stretch region in the TTD of UHRF2 can decrease the melting temperature of the TTD-PHD and represents a disordered region. Thus, these subtle but important mechanistic differences are potential avenues for selectively targeting the histone binding interactions of UHRF1 and UHRF2 with small molecules.

Shane M. Ginnard and Alyssa E. Winkler are the co-first authors.

1 | INTRODUCTION

Covalent modifications of histones such as acetylation, methylation, and ubiquitylation and the methylation of DNA form a complex epigenetic "language" that elicits a specific nuclear response such as transcriptional regulation or DNA repair.[1–5] This language is then "written" or "erased" by chromatin modifying enzymes that catalyze the addition or removal of covalent modifications. Histone posttranslational modifications (PTMs) are recognized by hundreds of different domains in epigenetic proteins, called "reader" proteins, in a site-specific manner and subsequently recruit nuclear machinery to chromatin to mediate a cellular output. Domains or modules in reader proteins include chromodomains, bromodomains, Tudor domains, and plant homeodomains (PHDs), which contain specialized pockets and cavities involved in recognition of their cognate histone PTMs.[2–4] In recent years, many of these reader domains have gained attention as novel therapeutic targets, as their aberrant binding to chromatin has been linked to the progression of various diseases including cancer.[6,7]

Ubiquitin-like containing PHD and ring finger (UHRF)1 and UHRF2 belong to a family of reader proteins that regulate epigenetic crosstalk between DNA methylation and histone modification via several chromatin interacting modules.[8–10] UHRF1 and UHRF2 share a high degree of sequence similarity and contain five functional domains called ubiquitin-like domain (UBL), tandem Tudor domain (TTD), PHD,

set and ring associated (SRA) domain, and really interesting new gene (RING) domain[9] (Figure 1A). Of the two proteins, UHRF1 is the most well characterized in terms of biological, structural, and biochemical function. Various studies have demonstrated that UHRF1 is critical for the recruitment of DNA methyltransferase 1 (DNMT1) to DNA replication forks in order to stimulate the methylation of daughter strands on hemimethylated substrates.[10–13] Detailed structural and mechanistic biochemical studies with the subdomains of UHRF1 have shown the TTD and PHD are histone reader domains that bivalently bind histone H3: the TTD interacts with histone 3 trimethylated lysine 9 (H3K9me3) and the PHD engages the first 4 amino acids of H3 including arginine 2 (H3R2).[14–18] This histone binding interaction allosterically enhances the binding of the SRA domain to DNA, whereby the hemimethylated DNA status stimulates the RING domain of UHRF1 to ubiquitinate multiple lysines on H3.[13,19] Both the ubiquitination of H3 and the physical interaction with UHRF1 facilitates the recruitment of DNMT1 to chromatin in order to catalyze maintenance methylation.[19,20]

Despite their high levels of sequence similarity, UHRF1 and UHRF2 appear to regulate discrete nuclear functions and demonstrate some mechanistic differences by which the reader/writer domains engage chromatin. For example, whereas UHRF1 plays a critical role in DNA methylation maintenance by recruiting DNMT1, UHRF2 is dispensable for this activity.[21,22] Similar to UHRF1, the TTD-PHD
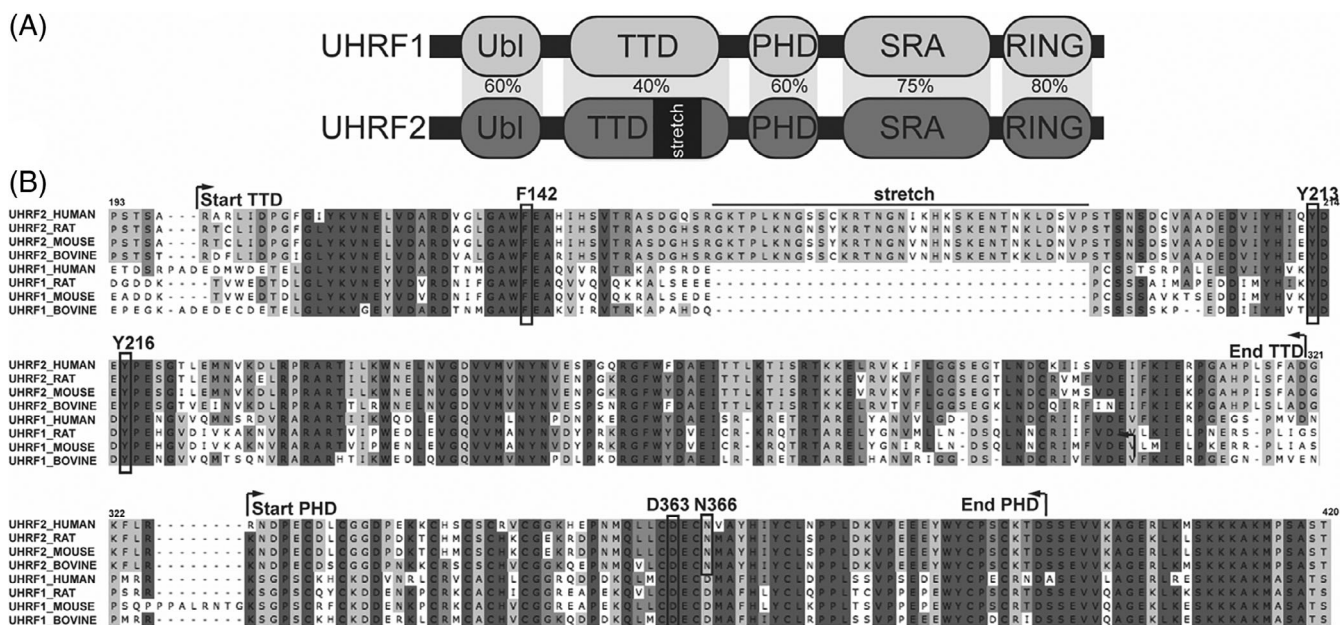
FIGURE 1 Domain Architecture of UHRF1 and UHRF2 and sequence alignment. (A) Schematic of UHRF 1 and UHRF2 domains and percent homology between them. (B) Primary amino acid sequence species alignment of TTD, and PHD domains of UHRF1 and UHRF2. Dark shade represents identity and lighter shades represent homology. KAlign software was used for the sequence alignments

histone binding module of UHRF2 binds K9me3 on the H3 tail and there is reciprocal allosteric activation of DNA and histone binding activities.[2,3] Both UHRF1 and UHRF2 ubiquitin ligase activity is stimulated by hemimethylated DNA on histone peptides, while only UHRF2 shows robust stimulation by hydroxymethylated DNA.[23] Notably, UHRF2 lacks the ability to ubiquitinate H3 on chromatin substrates,[23] which may explain the observation that UHRF2 is unable to rescue DNA methylation in embryonic stem cells lacking UHRF1.[21,22] Importantly, UHRF2 is a major regulator of hydroxymethylation, whereby reduced levels of UHRF2 is associated with lowered levels of hydroxymethylation in both developmental tissues and cancer.[24,25]

UHRF1 and UHRF2 also demonstrate distinct patterns of expression, particularly in cancer cells. For example, UHRF2 is upregulated in some differentiated cells such as vascular smooth muscle cells, while UHRF1 is downregulated during differentiation and overexpressed in embryonic stems cells.[22,25,26] UHRF1 is almost ubiquitously overexpressed in a variety of cancers including breast, prostate, colorectal, bladder, and lung cancer and its overexpression is often correlated with poor patient prognosis.[27–32] Overexpression of UHRF1 has been shown to downregulate the expression of tumor suppressor genes such as p16 and BRCA1 via hyper DNA methylation of promoters and aberrant histone methylation.[27,33–35] Thus, UHRF1 has been suggested to function as both a cancer biomarker and tumor promoter.[27]

Interestingly, UHRF2 appears to have opposing roles in cancer, depending on the type of cancer cell. For example, overexpression of UHRF2 has been shown to increase the epithelial mesenchymal transition in gastric cancer cell lines and promote tumor development via the Wnt/B-catenin signaling pathway.[36,37] UHRF2 was also found to be upregulated in colon cancer and its presence was associated with metastasis and poor prognosis.[38] However, other studies have found decreased levels or loss of UHRF2 in a variety of examined cancers tissues.[25,38–41] For example, low levels of UHRF2 was found in non-small cell lung cancer and this lowered expression was correlated with malignancy.[38] In esophageal squamous cell carcinoma (ESCC), UHRF2 expression was correlated with positive clinical outcomes and diminished epithelial–mesenchymal transition in ESCC cell lines.[39] In addition, UHRF2 has been shown to interact with many core proteins of the cell cycle network and has even been suggested to be a candidate tumor suppressor.[40,41]

Recently, there has been considerable interest in UHRF1 as a therapeutic target via inhibiting its DNA and histone reader function through small molecule inhibition.[8,42–46] In particular, several compounds have been identified using high throughput screening strategies that disrupt the histone binding activities of the TTD and TTD-PHD.[44–46] However, given the distinct cellular functions of UHRF1 and UHRF2 and their frequently dissimilar roles in cancer, each protein must be targeted without affecting the epigenetic reader function of the other. Thus, characterizing mechanistic differences in histone binding is a critical step toward developing selective UHRF1 and UHRF2 inhibitors.

To shed light on the histone binding differences between these two proteins, we have undergone a detailed biochemical and molecular investigation with the TTD, PHD and TTD-PHD domains of UHRF2 and performed a similar analysis with the UHRF1 counterpart. While UHRF1 and UHRF2 TTD-PHD have similar affinities toward H3K9me3, we show that UHRF2 TTD-PHD has higher selectivity for the trimethylated lysine 9. We determined the TTD of UHRF2 binds with modestly higher affinity toward the H3 tail when compared to the PHD, while the PHD was observed to be the main contributor of histone binding in UHRF1. We characterized critical residues that impart both affinity and selectivity in H3 tail engagement, which unveiled a distinct asparagine within the PHD of UHRF2 that weakens the histone binding interaction. Like UHRF1, the TTD and PHD domains of UHRF2 were found to cooperate in order to form high affinity interactions with the H3 tail. Lastly, we provide evidence that a unique, highly basic region of amino acids located within the TTD of UHRF2 is disordered. Thus, these mechanistic differences that we have discovered can be advantageously applied in a selective manner for future targeting the histone binding activities of UHRF1 and UHRF2.

2 | MATERIALS AND METHODS

2.1 | Peptides and synthesis

Peptides were purchased from New England Peptides or synthesized in house with amino acids purchased from Anaspec. The following are the sequences of fluorescein labeled peptides attached to a C-terminal lysine via an amide bond: H3K9me3-Fl (ARTKQTARK(Me3)STGG(K5Fam)) and H3unmod-Fl (ARTKQTARKSTGG(K5Fam). The following are the sequences of unlabeled peptides used for competition assays: H3K9me3 (ARTKQTARK(Me3)STGGK) and H3unmod (ARTKQTARKSTGGK). H3unmod-Fl was synthesized by solid phase peptide synthesis on a PS3 synthesizer from Protein Technologies, using rink amide MBHA resin as a solid support on a 0.1 mmol scale. The side chains of Ser and Thr were protected as the t-butyl derivative, Arg as the 2,2,5,7,8-pentamethyl-chroman-6-sulphonyl (Pmc), Gln as trityl (Trt), and His and Lys as the t-butyloxycarbonyl (Boc) form. Fluorenylmethoxycarbonyl (Fmoc)-protected amino acids were coupled in 4-fold excess with 2-(1H-benzotriazol-1-yl)-1,-1,3,3-tetramethyluronium hexafluorophosphate activating agent, and deprotection was accomplished by 20% piperidine in N,N-dimethylformamide. The peptide was cleaved from the resin using trifluoroacetic acid (TFA), distilled water, phenol, and triisopropylsilane, 88:5:5:2, for 2 h and precipitated with chilled diethyl ether followed by vacuum filtration, aqueous dissolution, and lyophilization. Purification was accomplished by reverse-phase HPLC using a Waters system and a 250×20 mm Higgins Analytical Proto300 C18 column, with a gradient of water (0.1% TFA) to acetonitrile (1% TFA) and monitoring at 220 nm. Purity was assessed by analytical HPLC on a Phenomenex C18 column (25 cm $\times$ 4.6 mm) at 220 nm. Molecular weight was determined using paper spray ionization mass spectrometry.

2.2 | DNA plasmids

Human UHRF2 TTD-PHD (127–394), UHRF2 TTD (113–323), UHRF2 PHD (324–394), UHRF1 TTD-PHD (133–366), UHRF1 TTD (126–286), and UHRF1 PHD (298–366) sequences were cloned into pGEX-KG, pET28b, or PHT4 (a derivative of pET15b [Novagen] vector plasmid), resulting in an N-terminal GST or His-tagged protein fusions. In general, GST-tagged protein constructs were used for fluorescence polarization and His-tagged protein constructs were used for thermal melt analysis.

2.3 | Mutagenesis and deletion constructs

Amino acid UHRF point mutants were created using the In-Fusion HD Cloning Plus System (Takara) or ordered from Genscript. The In-Fusion HD Cloning Plus System was also used to generate UHRF2 TTD Δ stretch and UHRF2 TTD-PHD Δ stretch constructs, which have amino acids 141–193 removed from the coding sequence. UHRF1 TTD + stretch was created by adding amino acids 141–193 from UHRF2 to UHRF1 TTD between amino acids 167 and 168.

2.4 | *E. coli* protein expression

For expression of pGEX-KG, pET28b and PHT4 vectors, Rosetta (DE3) *E. coli* cultures containing UHRF expression plasmids were grown in Fernbach flasks containing 1 liter of Luria Broth (LB) and antibiotics (100 μg/ml ampicillin and 25 μg/ml chloramphenicol) for ∼2 h at 37°C with shaking at 250 RPM. Once cell density reached an OD600 = 0.4–0.8, the cultures were induced with 0.2 mM IPTG for 16–20 h at 22°C. The cells pellets were harvested by centrifugation at 5000 RPM for 10 min at 22°C. *E. coli* expression of pET28b vectors in Rosetta was performed using similar procedures, with the exception of 20 μg/ml chloramphenicol and 50 μg/ml of kanamycin in the LB media.

2.5 | GST-tagged protein purification

Rosetta *E. coli* cell pellets expressing pGEX-KG constructs were lysed in 30 ml of Triton Lysis Buffer (50 mM Tris, pH 7.5, 150 mM NaCl, 10% glycerol, 0.5% Triton X-100, 1 mM BME) containing protease inhibitors (5 μg/ml aprotinin, 10 μg/ml leupeptin, 100 μM PMSF), 20 μg/ml DNAse I, and 10 μg/ml lysozyme. The cell lysate was centrifuged at 15,000 RPM for 30 min at 4°C. The resulting supernatant was passed over a gravity column containing 2.5 ml of glutathione agarose resin (Pierce) at 1 ml/min to capture the GST-tagged protein at 4°C. The resin was washed with 100 ml of Triton Lysis Buffer and eluted with 15 ml of GST Elution Buffer (50 mM Tris, pH 8.0, 10 mM reduced glutathione) at 1 ml/min. The eluent was dialyzed in Dialysis buffer (50 mM Tris, pH 7.5, 150 mM NaCl, 10% glycerol, 1 mM BME), and concentrated to 2 ml in Corning

Spin-X UF Concentrators (4°C), aliquoted into 100 μl volumes, snap frozen with liquid nitrogen and stored at −80°C. Samples from each step of the purification were visualized on SDS-PAGE gels to ensure >90% purity. The final protein concentration was determined using the Bio-Rad DC Protein Assay kit, according to the manufacturer's directions.

2.6 | His-tagged protein purification

Rosetta *E. coli* containing pET28b or pHT4 constructs were lysed and centrifuged as described under GST-tagged protein purification. The resulting supernatant was passed over a 5 ml Hi-Trap FF Crude column (GE) using a Biorad NGC 10 Chromatography System at 2 ml/min. The column was subsequently washed with 100 ml wash buffer (50 mM Tris, pH 7.5, 150 mM NaCl, 20 mM imidazole, 1 mM BME) and eluted with wash buffer containing 500 mM imidazole over a 15-column volume linear gradient. Dialysis, concentration, SDS-PAGE analysis, and protein quantitation was performed as described under GST-tagged protein purification.

2.7 | Fluorescence polarization

Binding saturation curves were performed as 100 μl reactions containing 50 mM Tris pH 7.5, 1 mg/ml BSA, 10 nM fluorescent histone peptide, 0–50 μM UHRF1/2 protein in 96-well black plates and incubated at ambient temperature with gentle shaking for 10 min. Each varied UHRF protein concentration was performed in triplicate or quadruplicate in the plate. The parallel and perpendicular fluorescence intensities of each plate well were subsequently read by a BioTek synergy platereader using $485/20_{em}$ and $528/20_{ex}$ filters with polarization. Millipolarization values were calculated using the following equation:

$$\text{Millipolarization} = \frac{I_{\parallel} - I_{\perp}}{I_{\parallel} + I_{\perp}} \cdot 1000 \tag{1}$$

where $I_{\perp}$ is the perpendicular intensity and $I_{\parallel}$ is the parallel intensity. These values were normalized such that the smallest mean value was defined as 0% and largest mean value was defined as 100% for each dataset. The data was then fit to Equation (2) to derive the dissociation constant (K_d) using Prism curve fitting software:

$$\text{Percent bound} = \frac{(\text{UHRF protein})}{K_d + (\text{UHRF protein})} \times C \tag{2}$$

where *C* is the *Y*-axis maximum (∼100%).

For competition assays, 100 μl reactions containing 50 mM Tris pH 7.5, 1 mg/ml BSA, 10 nM fluorescent histone peptide, (UHRF protein) resulting in 80% fraction bound, and 0–50 μM non-fluorescent competitor histone peptide were assembled into 96-well black plates and the millipolarization determined as described above. For graphing analysis, the competitor peptide

concentration was log transformed, millipolarization data normalized as described above and then fitted to the following Equation (3) in order to determine the IC_{50} value.

$$y = \left(1 + 10^{(\log IC50 - x) \times \text{hill slope}}\right) \quad (3)$$

2.8 | Sypro orange thermofluor assays

Forty-microliter reactions containing 12.5 mM sodium phosphate pH 7.5, 15× Sypro Orange (Invitrogen) and 60 μM His-tagged UHRF2 protein were assembled in white PCR strip tubes. For higher ionic strength conditions, 50 mM sodium phosphate pH 7.5, 150 mM NaCl, 15× Sypro Orange (Invitrogen), and 60 μM His-tagged UHRF2 protein was used instead. The strip tubes (8 replicates total) were placed in a BioRad Chrome4 qPCR thermocycler. A 10–95°C temperature gradient was used in which the temperature was increased 0.5° at 1-min intervals and fluorescence monitored at the ROX channel. The resulting fluorescence was normalized such that minimum fluorescence = 0% and the peak fluorescence intensity = 100%. The normalized data was then fit to Equation (4) to determine the melting temperature (T_m) as a handle of protein stability:

$$\text{Normalized fluorescence} = \frac{1}{1 + e^{(T_m - T)/c}} \times C \quad (4)$$

where T is temperature, and c is the slope factor. The T_m is the half maximal point in the melt curve.

2.9 | Differential scanning calorimetry

Six hundred-microliter volume containing 12.5 mM sodium phosphate pH 7.5, 60 μM His-tagged UHRF2 protein were loaded into the sample cell of a NanoDSC Model 6300 (TA Instruments). For higher ionic strength experiments, 600 μl volume containing 50 mM sodium phosphate pH 7.5, 150 mM NaCl, 60 μM His-tagged UHRF2 protein was loaded instead. The cell was heated from 20 to 80°C, at a rate of 1 degree minute and the heat change (kJ/mol K) was measured. Buffer control experiments were also conducted in order to perform baseline subtraction and the resulting data was fit to a Gaussian function in order to derive the T_m, which is the temperature at the peak of the thermal melting curve.

3 | RESULTS

3.1 | UHRF2 TTD-PHD has higher selectivity to H3K9me3 versus UHRF1 TTD-PHD

UHRF1 and UHRF2 contain TTD and PHD domains that are highly similar in primary amino acid sequence and domain architecture

(Figure 1A,B). In this study, we sought to determine mechanistic similarities and differences in histone binding by the two epigenetic reader domains. To measure the selectivity of the histone binding interaction with the tandemly linked TTD-PHD domains of UHRF2, we performed fluorescence polarization (FP) binding saturation assays to either fluorescein labeled H3K9me3 (H3K9me3-Fl) or H3 unmodified (H3unmod-Fl) peptides. Similar types of experiments were performed with UHRF1 TTD-PHD for comparison purposes. Consistent with a previous study, the TTD-PHD of UHRF2 selectively bound to H3K9me3-Fl ($K_d = 0.11$ μM) with ∼8-fold higher affinity over H3unmodified-Fl ($K_d = 0.85$ μM) (Figure 2A and Table 1).[23] Also consistent with the same study, the TTD-PHD of UHRF1 showed a modest ∼2.5-fold selectivity toward H3K9me3-Fl ($K_d = 0.22$ μM) over H3unmod-Fl ($K_d = 0.56$ μM) (Figure 2B and Table 1). Overall UHRF2 has higher selectivity for methylated lysine 9 compared to that of UHRF1.

To further demonstrate the selectivity of the interaction and to ensure the fluorophore attached to the C-terminus of the histones peptides does not interfere with binding, competition assays were undertaken in which unlabeled H3K9me3 and H3unmodified peptides were used to compete off the interaction between UHRF2 TTD-PHD and H3K9me3-Fl. UHRF2 TTD-PHD showed ∼7-fold higher affinity for H3K9me3 peptide ($IC_{50} = 0.18$ μM) versus the H3unmodified peptide ($IC_{50} = 1.15$ μM) (Figure 2C and Table 2). In contrast, UHRF1 TTD-PHD showed ∼2.5-fold higher affinity for H3K9me3 ($IC_{50} = 0.28$ μM) versus the H3unmodified peptide ($IC_{50} = 0.71$ μM), supporting the notion that UHRF1 is less selective for H3K9me3 in comparison to UHRF2 (Figure 2D and Table 2).

3.2 | Domain contributions to the H3 binding interaction

We next sought to determine the binding contribution of the TTD and PHD domains to the H3 tail interaction for UHRF2. To do so, we performed FP binding saturation assays with the isolated TTD and PHD to H3K9me3-Fl or H3unmod-Fl peptides. For comparison purposes, we also performed FP analyses with each histone binding domain of UHRF1, which revealed the PHD binds to H3K9me3-Fl ($K_d = 0.21$ μM) with similar affinity compared the TTD-PHD ($K_d = 0.22$ μM), while the TTD bound to the same peptide with much lower affinity ($K_d = 1.16$ μM) (Tables 1, 3, and 4). Thus consistent with a previous study, it appears that the PHD of UHRF1 is the primary contributor to histone binding.[47] In contrast, the TTD domain of UHRF2 ($K_d = 0.26$ μM) bound to H3K9me3-Fl ∼2-fold less compared to UHRF2 TTD-PHD ($K_d = 0.11$ μM) (Tables 1 and 3). Interestingly the PHD domain of UHRF2 ($K_d = 0.67$ μM) was found to contribute to the H3K9me3-Fl binding interaction ∼6-fold less compared to UHRF2 TTD-PHD ($K_d = 0.11$ μM) and ∼ 2.5-fold less compared to UHRF2 TTD ($K_d = 0.26$ μM). Thus, the TTD of UHRF2 has modestly higher affinity toward the H3 tail compared to the PHD, while the PHD of UHRF1 carries the bulk of the binding contribution.
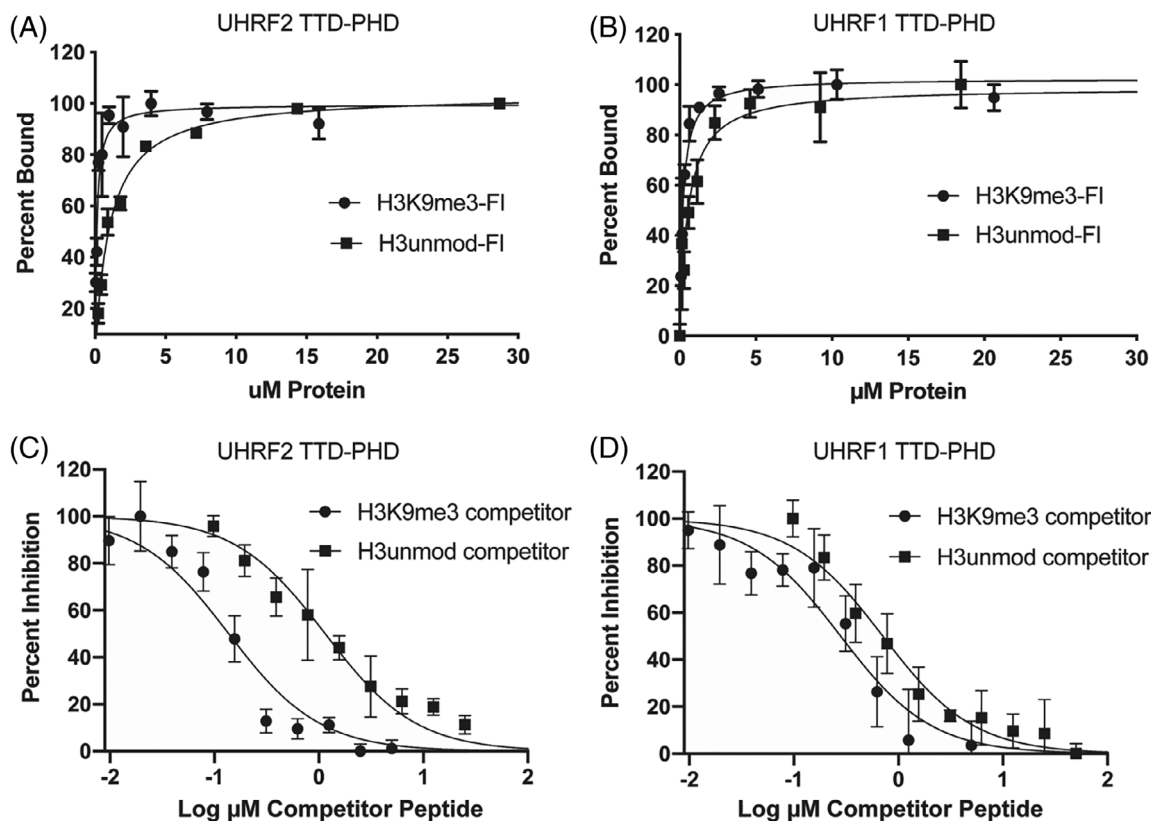
FIGURE 2 UHRF2 TTD-PHD is more selective for H3K9me3 compared to UHRF1 TTD-PHD. (A) Representative binding saturation assays with UHRF2 TTD-PHD with either H3K9me3-Fl ($K_d = 0.11$ μM) or H3unmod-Fl peptides ($K_d = 0.85$ μM). (B) Representative binding saturation assays with UHRF1 TTD-PHD with either H3K9me3-Fl ($K_d = 0.22$ μM) or H3unmod-Fl peptides ($K_d = 0.56$ μM). (C) Representative competition assays with UHRF2 TTD-PHD where H3K9me3-Fl is the binding peptide and H3K9me3 ($IC_{50} = 0.18$ μM) or H3unmod ($IC_{50} = 1.15$ μM) is the competitor peptide. (D) Representative competition assays with UHRF1 TTD-PHD where H3K9me3-Fl is the binding peptide and H3K9me3 ($IC_{50} = 0.28$ μM) or H3unmod ($IC_{50} = 0.71$ μM) is the competitor peptide

3.3 | Molecular basis for the H3K9me3 interaction within the TTD region of UHRF2

We next investigated the molecular basis by which the TTD of UHRF2 interacts with H3K9me3. It was previously demonstrated that a "cage" of aromatic amino acids (F152, Y188, and Y191) in UHRF1 form a cation–pi interaction with trimethylated lysine 9 on histone H3.[15–18] Sequence and structural alignments show a similar set of conserved aromatic amino acids (F144, Y213, Y216) that also form a cage within UHRF2 (Figures 1B, and 3A,B). To determine if these amino acids are critical for interacting with H3K9me3, single alanine mutants (F144A, Y213A, and Y216A) of UHRF2 were created in the context of TTD-PHD of UHRF2. UHRF2 TTD-PHD F144A ($K_d = 0.86$ μM), Y213A ($K_d = 1.12$ μM), and Y216A ($K_d = 1.33$ μM) showed ~8–10-fold loss of binding with H3K9me3-Fl compared to UHRF2 TTD-PHD ($K_d = 0.11$ μM) (Table 1). Similar K_d values with each of these mutants were observed with H3unmod-Fl, further highlighting their involvement with H3K9me3. Double (Y213A/216A) and triple (F144A/Y213A/Y216A) UHRF2 TTD-PHD aromatic acid mutants were also tested and showed further loss of binding with H3K9me3-Fl ($K_d = 5.09$ μM for Y213A/216A and $K_d = 18.69$ μM for F144A/Y213A/Y216A) and H3unmod-Fl ($K_d = 3.22$ μM for

Y213A/216A and $K_d = 9.29$ μM for F144A/Y213A/Y216A). To confirm the importance of the aromatic group, we also measured the binding interaction of a UHRF2 TTD-PHD Y216F mutant with H3K9me3-Fl ($K_d = 0.23$ μM) or H3unmod-Fl ($K_d = 0.90$ μM) and found little perturbation of binding compared to UHRF2 TTD-PHD WT.

To further isolate the role of the aromatic amino acids in UHRF2, mutational analysis was also performed with single domain TTD constructs. Fluorescence polarization binding analysis of all three UHRF2 TTD F144A, Y213A, and Y216A mutants showed complete ablation of binding with H3K9me3-Fl and H3unmodified-Fl peptides (Table 3). Together, these experiments demonstrate the critical importance of HK9me3 in engaging high affinity cation–pi interactions with aromatic amino acids located within the TTD domain of UHRF2.

In the context of UHRF1 TTD-PHD, we generated a similar set of aromatic cage mutants (Y191A and Y188A) for comparison and found that mutation of these residues did not significantly impact H3K9me3-Fl binding (UHRF1 TTD-PHD Y191A $K_d = 0.29$ μM and Y188A $K_d = 0.19$ μM vs. WT $K_d = 0.22$ μM). This is consistent with binding data from other groups that showed aromatic cage mutants (F152A, Y191A, and Y188A) within the context of UHRF1 TTD-PHD

TABLE 1 Dissociation constants (K_d) for UHRF TTD-PHD constructs with histone peptides

Construct	H3K9me3-Fl (µM)	H3unmod-Fl (µM)
UHRF1 TTD-PHD WT	0.22 ± 0.04	0.56 ± 0.14
UHRF1 TTD-PHD Y188A	0.29 ± 0.01	0.31 ± 0.01
UHRF1 TTD-PHD Y191A	0.19 ± 0.02	0.23 ± 0.01
UHRF1 TTD-PHD D334A	5.10 ± 1.37	NBD
UHRF1 TTD-PHD D337A	3.4 ± 0.3	9.04 ± 1.33
UHRF1 TTD-PHD D337N	1.9 ± 0.4	4.00 ± 1.20
UHRF1 TTD-PHD Y188A/ D334A	NBD	NBD
UHRF2 TTD-PHD WT	0.11 ± 0.04	0.85 ± 0.12
UHRF2 TTD-PHD F144A	0.86 ± 0.09	0.98 ± 0.08
UHRF2 TTD-PHD Y213A	1.12 ± 0.05	1.26 ± 0.01
UHRF2 TTD-PHD Y216A	1.33 ± 0.05	1.33 ± 0.07
UHRF2 TTD-PHD Y216F	0.23 ± 0.03	0.90 ± 0.07
UHRF2 TTD-PHD Y213A/ Y216A	5.09 ± 0.44	3.22 ± 0.18
UHRF2 TTD-PHD F144A/ Y213A/Y216A	18.69 ± 3.59	9.29 ± 0.91
UHRF2 TTD-PHD D363A	2.29 ± 0.64	NBD
UHRF2 TTD-PHD D363N	0.95 ± 0.06	NBD
UHRF2 TTD-PHD N366A	0.17 ± 0.01	0.94 ± 0.11
UHRF2 TTD-PHD N366K	3.67 ± 0.58	NBD
UHRF2 TTD-PHD N366D	0.18 ± 0.014	0.99 ± 0.07
UHRF2 TTD-PHD Y213A/ D363A	NBD	NBD
UHRF2 TTD-PHD Δ stretch	0.12 ± 0.02	1.06 ± 0.12

Note: NBD = no binding detected at the [protein] tested.

TABLE 2 Inhibition constants (IC_{50}) for UHRF TTD-PHD constructs with histone peptides

Construct	Competitor peptide	IC_{50} (µM)
UHRF1 TTD-PHD	H3K9me3	0.28 ± 0.03
UHRF1 TTD-PHD	H3unmodified	0.71 ± 0.05
UHRF2 TTD-PHD	H3K9me3	0.18 ± 0.01
UHRF2 TTD-PHD	H3unmodified	1.15 ± 0.05

Note: H3K9me3-Fl peptide was used as the UHRF binding partner.

TABLE 3 Dissociation constants (K_d) for UHRF TTD constructs with histone peptides

Construct	H3K9me3-Fl (µM)
UHRF1 TTD WT	1.16 ± 0.31
UHRF1 TTD Y188A	NBD
UHRF1 TTD Y191A	NBD
UHRF1 TTD + stretch	0.69 ± 0.09
UHRF2 TTD WT	0.26 ± 0.04
UHRF2 TTD Δ stretch	0.42 ± 0.12
UHRF2 TTD F144A	NBD
UHRF2 TTD Y213A	NBD
UHRF2 TTD Y216A	NBD

Note: No binding was detected with the H3unmod-Fl peptide for all UHRF1 and UHRF2 TTD constructs. NBD = no binding detected at the [protein] tested.

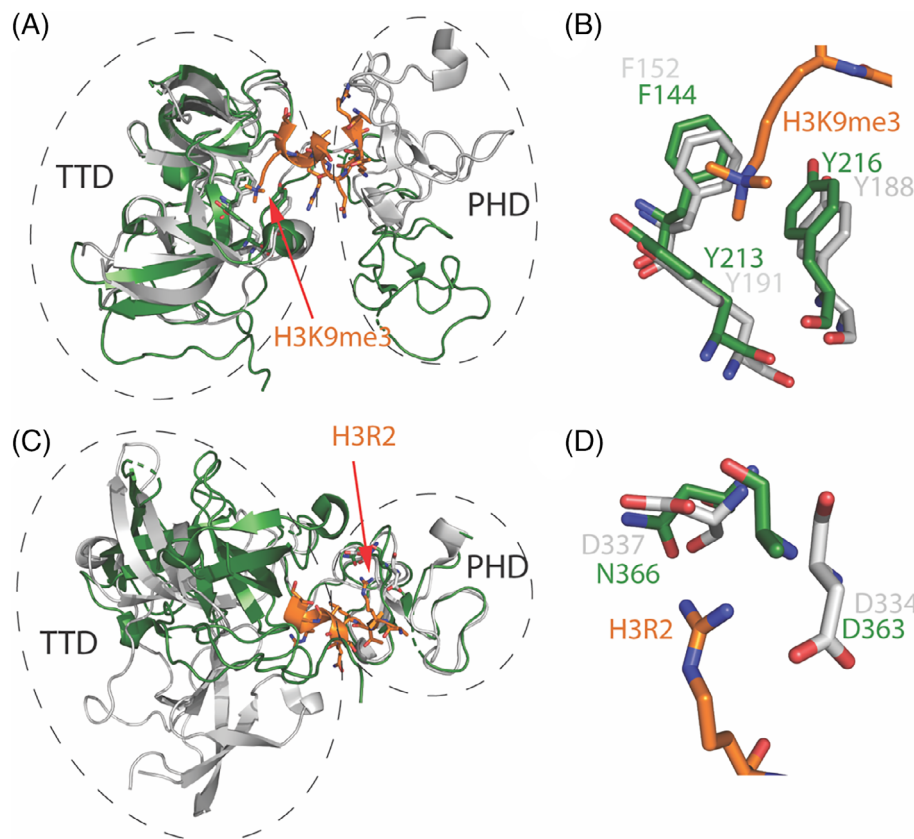**TABLE 4** Dissociation constants (K_d) for UHRF PHD constructs with histone peptides

Construct	H3K9me3-Fl (µM)	H3unmod-Fl (µM)
UHRF1 PHD WT	0.21 ± 0.06	0.22 ± 0.08
UHRF1 PHD D334A	NBD	NBD
UHRF1 PHD D337A	23.1 ± 3.8	14.2 ± 1.5
UHRF1 PHD D337N	1.3 ± 0.2	0.64 ± 0.13
UHRF2 PHD WT	0.67 ± 0.18	0.64 ± 0.29
UHRF2 PHD D363A	NBD	NBD
UHRF2 PHD D363N	NBD	NBD
UHRF2 PHD D363K	NBD	NBD
UHRF2 PHD N366A	NBD	NBD
UHRF2 PHD N366K	NBD	NBD
UHRF2 PHD N366D	0.15 ± 0.03	0.19 ± 0.06

Note: NBD = no binding detected at the [protein] tested.

affinity and can only partially compensate for binding when the TTD is mutated within the context of the TTD-PHD.

3.4 | Molecular basis of H3 binding with the PHD domain of UHRF2

We next investigated the molecular mechanism by which the PHD of UHRF2 interacts with histone H3. It was previously shown that D334 and D337 within the PHD of UHRF1 interact with R2 on histone H3 via ionic interactions.[14–16,18] Mutation of D334 to alanine in the PHD region of UHRF1 was shown to significantly disrupt binding to H3K9me3 peptide and this occurred to a somewhat lesser extent in D337A UHRF1 PHD to H3K9me3 peptide.[14,16] We also confirmed that D334 is a critical amino acid as D334A mutants in the context of UHRF1 TTD-PHD (K_d = 5.10 µM) and PHD (no binding detected) severely or completely diminished binding to H3K9me3-Fl (Tables 1 and 4). Analysis of UHRF1 TTD-PHD D337A (K_d = 3.4 µM) and

does not impair binding, probably due to full compensation of binding by the PHD.[16,23] The isolated UHRF1 TTD aromatic cage mutants (TTD Y191A and TTD Y188A) failed to show any binding to H3K9me3-Fl or H3unmod-Fl (Table 3), demonstrating that in the absence of the PHD, the aromatic amino acids are critical for associating with the H3 tail. These experiments also further support the notion that the PHD has the more critical role in maintaining H3 binding interactions versus the TTD for UHRF1. Such observations are distinct from those seen with UHRF2 where the PHD has lowered H3

FIGURE 3 Aligned crystal structures of UHRF1 TTD-PHD with H3K9me3 and apoUHRF2 TTD-PHD. (A) General alignment of UHRF1 TTD-PHD-H3K9me3 and apoUHRF2 TTD-PHD crystal structures. UHRF1 TTD-PHD is gray, UHRF2 TTD-PHD is green, and H3K9me3 peptide is orange. (B) Zoomed in view of the TTD aromatic cage of UHRF1 and UHRF2 that engage H3K9me3. (C) Alignment of PHDs with UHRF1 TTD-PHD-H3K9me3 and apoUHRF2 TTD-PHD crystal structures. (D) Zoomed in view of H3R2 binding site within the PHDs of UHRF1 and UHRF2. Side chain atoms of D363 in UHRF2 are disordered in the crystal structure. D334 of UHRF1 corresponds to D363 of UHRF2. UHRF2 PDB ID is 4TVR. UHRF1 PDB ID is 4GY5.[16] PyMOL structure visualization software was used to create structure representations

UHRF1 PHD D337A (K_d = 23.1 μM) mutants also confirmed loss of binding to H3K9me3-Fl. As expected, since the PHD does not associate with K9me3, similarly affinity values with these mutants were determined toward H3unmod-Fl (Tables 1 and 4).

A global overlay of the crystal structures of UHRF1 TTD-PHD in complex with H3K9me3 peptide (PDB ID: 4GY5)[16] and apo UHRF2 TTD-PHD (PDB ID: 4TVR) show a high degree of alignment of the TTD domain, whereas the PHDs do not appear to align (Figure 3A). However, overlay of just the PHDs of UHRF1 and UHRF2 reveals the PHDs are actually structurally similar, whereas the TTDs do not align (Figure 3C). Thus, it appears that both the TTDs and PHDs are structurally very similar, and the arrangement of the linker region that connects the TTD and PHD is different, possibly due to presence or absence of bound H3 ligand. A closer look at the potential R2 H3 binding site in the overlayed PHD structures shows that for UHRF2, D363 is invariant (the analogous amino acid is D334 in UHRF1), while interestingly, UHRF2 contains an asparagine (N366) at the corresponding D337 position in UHRF1 (Figure 3D). D334 and D337 of UHRF1 were previously shown to form electrostatic interactions with H3R2.[14-16,18] Thus, the PHD overlay structures suggest that N366 in the H3R2 binding site might reduce the electrostatic interactions between the PHD of UHRF2 and H3 and thereby weaken the binding interaction.

To study the importance of UHRF2 D363 in histone binding, the amino acid residue was mutated to alanine, lysine, or asparagine and the ability of the mutants to bind to H3K9me3 was tested within the context of UHRF2 TTD-PHD and PHD alone. Mutation of UHRF2

TTD-PHD D363 to N (K_d = 0.95 μM) or A (K_d = 2.29 μM) significantly disrupted the ability of the TTD-PHD to bind to H3K9me3-Fl ~10–20-fold, respectively, compared to WT UHRF2 TTD-PHD (K_d = 0.11 μM) (Table 1). As expected, since the PHD is unlikely to interact with K9me3, similar affinity values with these mutants were determined toward H3unmod-Fl (Table 1). Since the presence of the TTD within the TTD-PHD construct likely provides some of the remaining histone binding interaction observed in mutants, binding analysis was performed in the context of UHRF2 single domain mutants in order to isolate the role of this amino acid within the PHD. Indeed, no binding was observed with D363A, D363N, D363K single domain PHD mutants with either H3K9me3-Fl or H3unmod-Fl (Table 4). The lack of histone binding regardless of the type of mutation suggests D363 has a critical role in interacting with the histone tail.

Mutational analysis was also performed to interrogate the role of N366 in histone binding. N366A, N366D, and N366K mutants were created in the context of the UHRF2 TTD-PHD and PHD isolated domain. UHRF2 TTD-PHD N366A (K_d = 0.17 μM) and N366D (K_d = 0.18 μM) mutants showed similar affinity values compared to WT UHRF2 TTD-PHD (K_d = 0.11 μM). Only the UHRF2 TTD-PHD N366K mutant (K_d = 3.67 μM) showed a significant loss of binding. Assuming that N366 may be within interaction distance of R2 of H3, the perturbation of binding may be due to a strong electrostatic repulsion between N366K of UHRF2 and R2 of H3.

Within the context of the isolated PHD domain, no binding was observed for N366A and N366K UHRF2 PHD mutants (Table 4). Interestingly, the UHRF2 PHD N366D mutant (K_d = 0.15 μM) showed

a ~4.5-fold enhancement of binding compared to WT UHRF2 PHD (K_d = 0.67 µM). Notably, this binding affinity is similar to that of UHRF1 PHD (K_d = 0.21 µM). One possible explanation for this observation is the change of asparagine to aspartate in UHRF2 recapitulates the electrostatic binding interaction between D337 of UHRF1 and R2 of H3. To test the hypothesis that N366 in the UHRF2 PHD weakens the H3 interaction, we created D337N substitutions in both UHRF1 TTD-PHD and UHRF1 PHD and measured their ability to bind to H3K9me3-Fl. Indeed, both UHRF1 TTD-PHD D337N (K_d = 1.9 µM) and UHRF1 PHD D337N (K_d = 1.9 µM) showed ~5–10-fold loss of binding compared to their WT counterparts (Table 1). Together, the mutational analysis suggests that N366 in UHRF2 weakens the binding affinity of the PHD to the histone tail compared to UHRF1 due to a reduced electrostatic interaction. By doing so, this property precludes the PHD from being the main contributor to the histone binding interaction.

3.5 | Specific amino acids within the TTD and PHD domains of UHRF2 cooperate to bind the H3 tail

The above results highlight an interesting interaction between H3 and the TTD-PHD of UHRF2; mutation of one domain within the context of the double domain only partially disrupts the binding interaction while mutation within the single domain completely abrogates binding. Such phenomena suggest that both domains work together to bind the H3 tail. Indeed, coordinating binding properties have previously been demonstrated with the both UHRF1 and UHRF2 TTD-PHD.[15,16,18,23] To further confirm the cooperative nature of the histone binding interaction, we tested the ability of both UHRF1 TTD-PHD D334A and UHRF2 TTD-PHD D363A to bind to H3unmod-Fl. Similar to a previous study,[23] neither UHRF1 TTD-PHD D334A nor UHRF2 TTD-PHD D363A showed any detectable binding to H3ummod-Fl (Table 1).

We next investigated whether the aromatic amino acids in the TTD and D363 in the PHD of UHRF2 are both specifically critical for dual domain H3 engagement. To test this possibility, UHRF2 mutants were created in which both of these amino acid residues within the TTD and PHD domains of UHRF2 were mutated in the context of the double domain construct (UHRF2 TTD-PHD Y213A/D363A) and its ability to interact with H3K9me3-Fl tested. Similar to the above studies, this mutant failed to demonstrate any binding activity with H3K9me3-Fl and a similar lack of binding phenomena was also observed with the UHRF1 TTD-PHD F188A/D334A double mutant (Table 1). Together, these studies support the model that the TTD and PHD domains of both UHRF1 and UHRF2 cooperate and that dual domain engagement relies on the interactions of specific amino acid residues with the H3 tail.

3.6 | The stretch region UHRF2 is not required for histone binding and is likely disordered

Alignment of the amino acid sequence of the TTD-PHD of UHRF1 and UHRF2 shows a unique ~35 amino acid insertion within the TTD

of UHRF2, coined the "TTD stretch" (Figure 1A,B).[22] Interestingly, this region of UHRF2 is highly conserved among various species. To interrogate the role of this region in histone binding, we removed this portion from UHRF2 TTD (UHRF2 TTD Δ stretch) and UHRF2 TTD-PHD (UHRF2 TTD-PHD Δ stretch) and measured the ability of these constructs to bind histone H3. We found little perturbation of binding to H3K9me3-Fl with UHRF2 TTD Δ stretch (K_d = 0.42 µM) or UHRF2 TTD-PHD Δ stretch (K_d = 0.12 µM) versus their WT counterparts (Tables 1 and 3). In addition, both UHRF2 TTD Δ stretch (no binding detected) and UHRF2 TTD-PHD Δ stretch (K_d = 1.06 µM) interacted with H3unmod-Fl to a similar extent compared to WT UHRF2 constructs. Thus, the stretch region of UHRF2 is dispensable for histone binding and appears to have some other functional role in the protein. To further characterize the histone binding role of the stretch region of the TTD in UHRF2, we performed a "swap" experiment by inserting this region of UHRF2 into the TTD of UHRF1 (UHRF1 TTD + stretch). FP analysis with UHRF1 TTD + stretch (K_d = 0.69 µM) demonstrated negligible H3K9me3-Fl binding differences compared to UHRF1 TTD (K_d = 1.16 µM) (Table 3). The lack of significant differences in binding affinities further argues against a clear role of the stretch region in directly binding to histone H3.

We next performed various sequence analyses of the stretch region in order to gain further insight into its structure and function. Intriguingly, the stretch region is rich in arginine and lysine amino acids and has an isoelectric point of ~10. Given that nuclear localization sequences (NLS) also tend to be concentrated with basic amino acids, we analyzed the sequence of UHRF2 through several NLS predictive software tools, including NucPred, NLStradamus, and SeqNLS.[48–50] However, not only did the analyses not identify an NLS in the stretch region, no NLSs were detected throughout the entire sequence of UHRF2.

Disordered regions in proteins are often low in hydrophobicity and contain a high degree of negatively or positively charged amino acids.[51–54] Given its highly basic nature, we next considered the possibility that the stretch region may be disordered. Analysis of UHRF2 via GlobPlot and DISOPRED protein sequence analysis servers predicted the stretch region as disordered (Figure S1).[55,56] Lending support to this notion, the stretch region is not visible within crystal structure of UHRF2 TTD-PHD (PDB:4TVR).

If the stretch region is indeed disordered, then removal of the stretch region is likely to improve the thermal stability of UHRF2. To test this possibility, Sypro Orange ThermoFluor assays were performed to determine the melting temperature (T_m) of UHRF2 TTD Δ stretch and UHRF2 TTD-PHD Δ stretch and compared to its WT counterparts. UHRF2 TTD Δ stretch (T_m = 34.7°C) showed no difference in thermal stability compared to WT UHRF2 TTD (T_m = 34.2°C) (Figure 4A). Interestingly, there was a modest, but significant ($p < .0001$) enhancement of the melting temperature of UHRF2 TTD-PHD Δ stretch (T_m = 43.5°C) compared to WT UHRF2 TTD-PHD (T_m = 41.9°C) (Figure 4B). To ensure that these differences in melting temperatures were not due to dye access effects, we also used differential scanning calorimetry (DSC) to measure the melting temperatures of both TTD-PHD constructs based on temperature-dependent heat changes.

Consistent with the dye-based assay, UHRF2 TTD-PHD Δ stretch (T_m = 46.8°C) demonstrated a higher melting temperature compared to WT UHRF2 TTD-PHD (T_m = 45.0°C) using DSC (Figure 4D).

A common property of either a highly acidic or basic disordered region is its stabilization at higher salt concentrations due to the shielding effects of the ions with the charged groups.[53,54] We next tested whether the TTD-PHD of UHRF2 might also exhibit such phenomena with increasing the ionic strength. In agreement with this notion, the melting temperature of UHRF2 TTD-PHD (T_m = 42.9°C) shifted upwards toward that of UHRF2 TTD-PHD Δ stretch (T_m = 43.6°C) at higher ionic strength conditions in the ThermoFluor assays (Figure 4C). DSC experiments also revealed the melting temperatures of the TTD-PHD (T_m = 46.1°C) to nearly converge to that of TTD-PHD Δ stretch (T_m = 46.5°C) at higher ionic strength conditions, indicating that the presence of salts may be shielding the basic groups on the stretch and stabilizing it (Figure 4E). Together, these data provide support toward the model that the unique stretch of amino acids present in UHRF2 and absent in UHRF1 is a disordered region.

4 | DISCUSSION

Previous studies have characterized the histone binding properties of the TTD-PHD of UHRF2 under equilibrium conditions and the isolated TTD and PHD domains under nonequilibrium conditions.[22,23] However, this study represents the first detailed quantitative binding analysis with the isolated TTD and PHD domains and TTD-PHD of UHRF2 together under equilibrium conditions in order to better understand their function in histone binding. In doing so, we have uncovered subtle, but key differences in the molecular selectivity, affinity and domain binding contributions to the H3 tail compared to UHRF1.

We sought to determine differences in binding contributions between the TTD and PHD in both UHRF1 and UHRF2. Consistent with another study,[47] we found that the PHD of UHRF1 provides the bulk of the high affinity interaction toward H3. Also similar to others,[16,23] we showed that the aromatic cage of amino acids within the TTD of UHRF1 provides some binding selectivity toward H3K9me3, but is not necessary for maintaining high affinity interactions in the context of the TTD-PHD. This is likely due to the fact that the PHD of UHRF1 is the main contributor to H3 binding via D334 and D337 forming strong electrostatic interactions with R2 of H3 (Figure 3D). In this study, we unveiled the novel finding that the TTD of UHRF2 has modestly higher affinity toward the H3 tail that is trimethylated at K9, compared to the PHD which has a weaker binding interaction. This difference in the binding contribution between TTD and PHD domains in UHRF2 is at least partially attributed to a distinct molecular interaction observed in the R2 binding pocket of
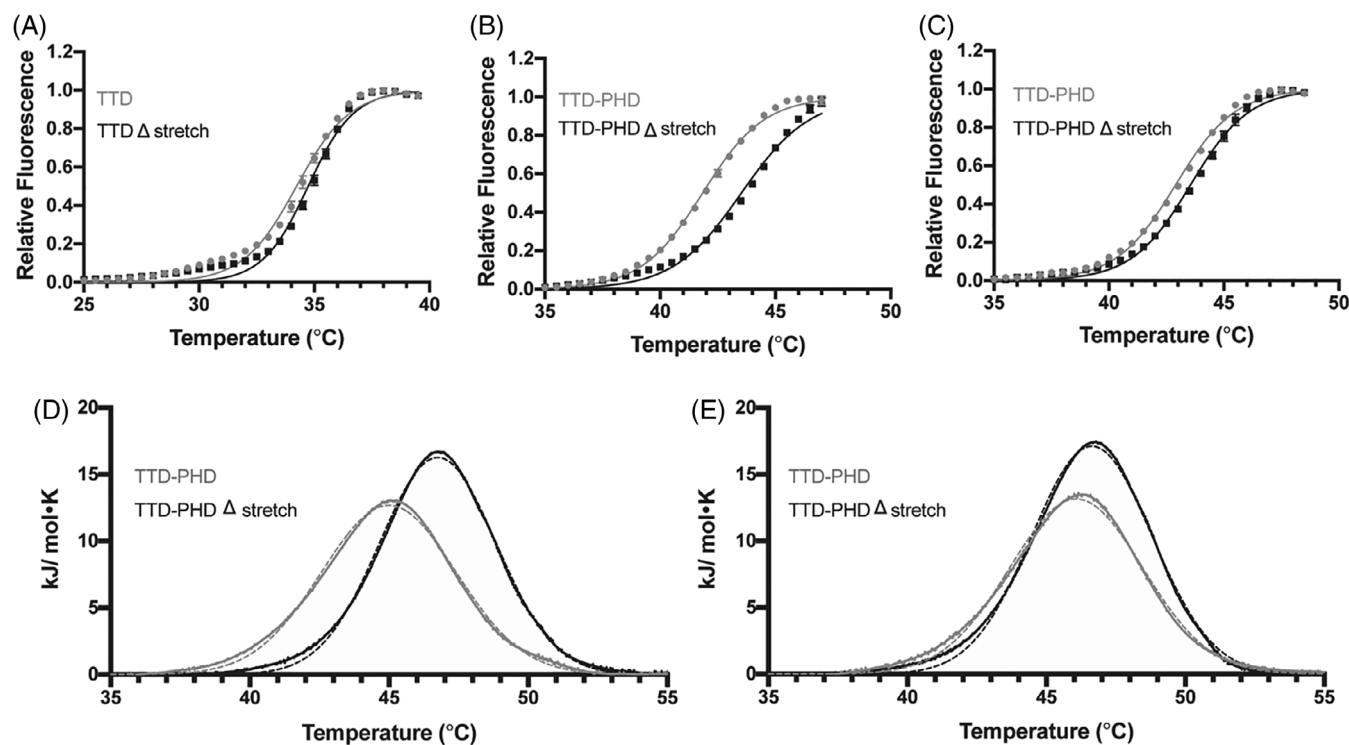
FIGURE 4 ThermoFluor and DSC analyses of UHRF2. (A) ThermoFluor assays with UHRF2 TTD (T_m = 34.2°C) and UHRF2 TTD Δ stretch (T_m = 34.7°C). (B) ThermoFluor assays with UHRF2 TTD-PHD (T_m = 41.9°C) and UHRF2 TTD-PHD Δ stretch (T_m = 43.5°C). (C) ThermoFluor assays with UHRF2 TTD-PHD (T_m = 42.9°C) and UHRF2 TTD-PHD Δ stretch (T_m = 43.6°C) at higher ionic strength conditions. (D) DSC analyses with UHRF2 TTD-PHD (T_m = 45.0°C) and UHRF2 TTD-PHD Δ stretch (T_m = 46.8°C). (E) DSC analysis with UHRF2 TTD-PHD (T_m = 46.1°C) and UHRF2 TTD-PHD Δ stretch (T_m = 46.5°C) at higher ionic strength conditions. Data fit to Gaussian function are dashed lines in the DSC experiments

H3. While UHRF1 contains two aspartates within the PHD, UHRF2 has an aspartate (D363) and an asparagine (N366) in the analogous positions. The presence of asparagine in the H3R2 binding pocket of UHRF2 lowers the electrostatic binding potential between the PHD and H3. As a result, the aromatic amino acids within the TTD of UHRF2 take on greater importance in engaging the H3 tail and offer a higher degree of selectivity for H3K9me3 interaction within the context of the TTD-PHD (Figure 3B). Consistent with this data, we found that mutating the aromatic residues within the context of the TTD-PHD of UHRF2 greatly reduced its binding affinity toward H3K9me3, due to the fact that PHD cannot provide full binding compensation.

In agreement with previous studies,[15,16,18,23] we confirmed and provided support to the notion that TTD and PHD domains in both UHRF1 and UHRF2 cooperate in order to bind to H3. Here, we have further built upon those studies to demonstrate that the aromatic amino acids with the TTD and D363 (UHRF2)/D334 (UHRF1) within the PHD are the critical amino acids residues necessary for cooperative engagement by both domains.

We performed a preliminary characterization of the structural and biophysical properties of the stretch region, a string of ~35 amino acids present within the TTD of UHRF2 and absent in UHRF1. Given that removing the stretch region did not alter binding affinity of UHRF2 TTD and TTD-PHD to H3K9me3, we hypothesized that it does not directly interact with H3, but has some other functional role in the protein. Since sequence analysis of UHRF2 predicted the stretch region to be disordered, we tested if removal of the stretch region had any effect on the thermal stability of UHRF2. Indeed, TTD-PHD Δ stretch exhibited higher melting temperatures compared to WT TTD-PHD in a low ionic strength condition. Distinctive of a highly positive charged disordered region,[53,54] we found that increasing the ionic strength enhanced the thermal stability of UHRF2 TTD-PHD, likely due to shielding effects of the anions from the salt with the basic groups within the stretch. Interestingly, no T_m differences were observed between UHRF2 TTD and UHRF2 TTD Δ stretch, possibly implying that the PHD of UHRF2 may influence the structural dynamics of the stretch region.

The exact functional role of the stretch in UHRF2 remains unclear. Often, disordered regions in proteins mediate protein–protein interactions or are sites of PTM.[57–60] It is tempting to hypothesize that the stretch region mediates electrostatic interactions with nucleosomal DNA or that its basic residues may be subject to PTMs such as acylation or methylation, which could impact overall charge and level of disorder. Future experiments should focus on understanding how the disordered state of the stretch is regulated, how the PHD of UHRF2 affects the structural dynamics of the stretch region and the functional role of the stretch region in cells.

Recently, there has been great interest in identifying compounds that target UHRF1 as potential anticancer agents.[42–46] The mechanism of action of several of these compounds involves disrupting the histone binding activities of the TTD or TTD-PHD domains.[44–46] However, given the distinct cellular and cancer-associated functions of UHRF1 and UHRF2, careful consideration should be given in selectively targeting one protein without affecting the epigenetic reader function of the other. Our findings illustrating the nuances of UHRF1 and UHRF2 H3 tail recognition by the TTD and PHD domains and the structural properties and dynamics of the stretch region in UHRF2 will inform the rationale design of compounds that selectively target these proteins.

PEER REVIEW

The peer review history for this article is available at https://publons.com/publon/10.1002/prot.26278.

DATA AVAILABILITY STATEMENT

The data that support the findings of this study are available from the corresponding author upon reasonable request.

ORCID

Brittany N. Albaugh https://orcid.org/0000-0001-6416-3800

REFERENCES

1. Bannister AJ, Kouzarides T. Regulation of chromatin by histone modifications. *Cell Res*. 2011;21(3):381-395. doi:10.1038/cr.2011.22
2. Musselman CA, Lalonde M-E, Côté J, Kutateladze TG. Perceiving the epigenetic landscape through histone readers. *Nat Struct Mol Biol*. 2012;19(12):1218-1227. doi:10.1038/nsmb.2436
3. Rothbart SB, Strahl BD. Interpreting the language of histone and DNA modifications. *Biochim Biophys Acta*. 2014;1839(8):627-643. doi:10.1016/j.bbagrm.2014.03.001
4. Taverna SD, Li H, Ruthenburg AJ, Allis CD, Patel DJ. How chromatin-binding modules interpret histone modifications: lessons from professional pocket pickers. *Nat Struct Mol Biol*. 2007;14(11):1025-1040. doi:10.1038/nsmb1338
5. Su Z, Denu JM. Reading the combinatorial histone language. *ACS Chem Biol*. 2016;11(3):564-574. doi:10.1021/acschembio.5b00864
6. Mio C, Bulotta S, Russo D, Damante G. Reading cancer: chromatin readers as druggable targets for cancer treatment. *Cancers (Basel)*. 2019;11(1):61–78. doi:10.3390/cancers11010061
7. Cheng Y, He C, Wang M, et al. Targeting epigenetic regulators for cancer therapy: mechanisms and advances in clinical trials. *Sig Transduct Target Ther*. 2019;4(1):1-39. doi:10.1038/s41392-019-0095-0
8. Bronner C, Achour M, Arima Y, Chataigneau T, Saya H, Schini-Kerth VB. The UHRF family: oncogenes that are drugable targets for cancer therapy in the near future? *Pharmacol Ther*. 2007;115(3):419-434. doi:10.1016/j.pharmthera.2007.06.003
9. Hashimoto H, Horton JR, Zhang X, Cheng X. UHRF1, a modular multidomain protein, regulates replication-coupled crosstalk between DNA

methylation and histone modifications. *Epigenetics*. 2009;4(1):8-14. doi:10.4161/epi.4.1.7370

10. Bronner C, Alhosin M, Hamiche A, Mousli M. Coordinated dialogue between UHRF1 and DNMT1 to ensure faithful inheritance of methylated DNA patterns. *Genes (Basel)*. 2019;10(1):65–78. doi:10.3390/genes10010065

11. Sharif J, Muto M, Takebayashi S, et al. The SRA protein Np95 mediates epigenetic inheritance by recruiting Dnmt1 to methylated DNA. *Nature*. 2007;450(7171):908-912. doi:10.1038/nature06397

12. Bostick M, Kim JK, Estève P-O, Clark A, Pradhan S, Jacobsen SE. UHRF1 plays a role in maintaining DNA methylation in mammalian cells. *Science*. 2007;317(5845):1760-1764. doi:10.1126/science.1147939

13. Liu X, Gao Q, Li P, et al. UHRF1 targets DNMT1 for DNA methylation through cooperative binding of hemi-methylated DNA and methylated H3K9. *Nat Commun*. 2013;4(1):1563. doi:10.1038/ncomms2562

14. Hu L, Li Z, Wang P, Lin Y, Xu Y. Crystal structure of PHD domain of UHRF1 and insights into recognition of unmodified histone H3 arginine residue 2. *Cell Res*. 2011;21(9):1374-1378. doi:10.1038/cr.2011.124

15. Arita K, Isogai S, Oda T, et al. Recognition of modification status on a histone H3 tail by linked histone reader modules of the epigenetic regulator UHRF. *Proc Natl Acad Sci U S A*. 2012;109(32):12950-12955. doi:10.1073/pnas.1203701109

16. Cheng J, Yang Y, Fang J, et al. Structural insight into coordinated recognition of trimethylated histone H3 lysine 9 (H3K9me3) by the plant homeodomain (PHD) and tandem Tudor domain (TTD) of UHRF1 (ubiquitin-like, containing PHD and RING finger domains, 1) protein. *J Biol Chem*. 2013;288(2):1329-1339. doi:10.1074/jbc.M112.415398

17. Nady N, Lemak A, Walker JR, et al. Recognition of multivalent histone states associated with heterochromatin by UHRF1 protein. *J Biol Chem*. 2011;286(27):24300-24311. doi:10.1074/jbc.M111.234104

18. Xie S, Jakoncic J, Qian C. UHRF1 double Tudor domain and the adjacent PHD finger act together to recognize K9me3-containing histone H3 tail. *J Mol Biol*. 2012;415(2):318-328. doi:10.1016/j.jmb.2011.11.012

19. Harrison JS, Cornett EM, Goldfarb D, et al. Hemi-methylated DNA regulates DNA methylation inheritance through allosteric activation of H3 ubiquitylation by UHRF1. Workman JL, ed. *eLife*. 2016;5:e17101. doi:10.7554/eLife.17101

20. Ishiyama S, Nishiyama A, Saeki Y, et al. Structure of the Dnmt1 reader module Complexed with a unique two-mono-ubiquitin mark on histone H3 reveals the basis for DNA methylation maintenance. *Mol Cell*. 2017;68(2):350-360.e7. doi:10.1016/j.molcel.2017.09.037

21. Zhang J, Gao Q, Li P, et al. S phase-dependent interaction with DNMT1 dictates the role of UHRF1 but not UHRF2 in DNA methylation maintenance. *Cell Res*. 2011;21(12):1723-1739. doi:10.1038/cr.2011.176

22. Pichler G, Wolf P, Schmidt CS, et al. Cooperative DNA and histone binding by Uhrf2 links the two major repressive epigenetic pathways. *J Cell Biochem*. 2011;112(9):2585-2593. doi:10.1002/jcb.23185

23. Vaughan RM, Dickson BM, Cornett EM, Harrison JS, Kuhlman B, Rothbart SB. Comparative biochemical analysis of UHRF proteins reveals molecular mechanisms that uncouple UHRF2 from DNA methylation maintenance. *Nucleic Acids Res*. 2018;46(9):4405-4416. doi:10.1093/nar/gky151

24. Chen R, Zhang Q, Duan X, et al. The 5-Hydroxymethylcytosine (5hmC) reader UHRF2 is required for Normal levels of 5hmC in mouse adult brain and spatial learning and memory. *J Biol Chem*. 2017;292(11):4533-4543. doi:10.1074/jbc.M116.754580

25. Lu H, Bhoopatiraju S, Wang H, et al. Loss of UHRF2 expression is associated with human neoplasia, promoter hypermethylation, decreased 5-hydroxymethylcytosine, and high proliferative activity. *Oncotarget*. 2016;7(46):76047-76061. doi:10.18632/oncotarget.12583

26. Luo T, Cui S, Bian C, Yu X. Uhrf2 is important for DNA damage response in vascular smooth muscle cells. *Biochem Biophys Res Commun*. 2013;441(1):65-70. doi:10.1016/j.bbrc.2013.10.018

27. Ashraf W, Ibrahim A, Alhosin M, et al. The epigenetic integrator UHRF1: on the road to become a universal biomarker for cancer. *Oncotarget*. 2017;8(31):51946-51962. doi:10.18632/oncotarget.17393

28. Geng Y, Gao Y, Ju H, Yan F. Diagnostic and prognostic value of plasma and tissue ubiquitin-like, containing PHD and RING finger domains 1 in breast cancer patients. *Cancer Sci*. 2013;104(2):194-199. doi:10.1111/cas.12052

29. Babbio F, Pistore C, Curti L, et al. The SRA protein UHRF1 promotes epigenetic crosstalks and is involved in prostate cancer progression. *Oncogene*. 2012;31(46):4878-4887. doi:10.1038/onc.2011.641

30. Unoki M, Daigo Y, Koinuma J, Tsuchiya E, Hamamoto R, Nakamura Y. UHRF1 is a novel diagnostic marker of lung cancer. *Br J Cancer*. 2010;103(2):217-222. doi:10.1038/sj.bjc.6605717

31. Kofunato Y, Kumamoto K, Saitou K, et al. UHRF1 expression is upregulated and associated with cellular proliferation in colorectal cancer. *Oncol Rep*. 2012;28(6):1997-2002. doi:10.3892/or.2012.2064

32. Unoki M, Kelly JD, Neal DE, Ponder BAJ, Nakamura Y, Hamamoto R. UHRF1 is a novel molecular marker for diagnosis and the prognosis of bladder cancer. *Br J Cancer*. 2009;101(1):98-105. doi:10.1038/sj.bjc.6605123

33. Unoki M, Nishidate T, Nakamura Y. ICBP90, an E2F-1 target, recruits HDAC1 and binds to methyl-CpG through its SRA domain. *Oncogene*. 2004;23(46):7601-7610. doi:10.1038/sj.onc.1208053

34. Jin W, Chen L, Chen Y, et al. UHRF1 is associated with epigenetic silencing of BRCA1 in sporadic breast cancer. *Breast Cancer Res Treat*. 2010;123(2):359-373. doi:10.1007/s10549-009-0652-2

35. Alhosin M, Omran Z, Zamzami MA, et al. Signalling pathways in UHRF1-dependent regulation of tumor suppressor genes in cancer. *J Exp Clin Cancer Res*. 2016;35(1):174. doi:10.1186/s13046-016-0453-5

36. Lai M, Liang L, Chen J, et al. Multidimensional proteomics reveals a role of UHRF2 in the regulation of epithelial–mesenchymal transition (EMT). *Mol Cell Proteomics*. 2016;15(7):2263-2278. doi:10.1074/mcp.M115.057448

37. Li L, Duan Q, Zeng Z, et al. UHRF2 promotes intestinal tumorigenesis through stabilization of TCF4 mediated Wnt/β-catenin signaling. *Int J Cancer*. 2020;147(8):2239-2252. doi:10.1002/ijc.33036

38. Lu S, Yan D, Wu Z, et al. Ubiquitin-like with PHD and ring finger domains 2 is a predictor of survival and a potential therapeutic target in colon cancer. *Oncol Rep*. 2014;31(4):1802-1810. doi:10.3892/or.2014.3035

39. Iguchi T, Ueda M, Masuda T, et al. Identification of UHRF2 as a negative regulator of epithelial–mesenchymal transition and its clinical significance in esophageal squamous cell carcinoma. *OCL*. 2018;95(3):179-187. doi:10.1159/000488860

40. Mori T, Ikeda DD, Yamaguchi Y, Unoki M, NIRF Project, eds. NIRF/UHRF2 occupies a central position in the cell cycle network and allows coupling with the epigenetic landscape. *FEBS Lett*. 2012;586(11):1570-1583. doi:10.1016/j.febslet.2012.04.038

41. Mori T, Ikeda DD, Fukushima T, Takenoshita S, Kochi H. NIRF constitutes a nodal point in the cell cycle network and is a candidate tumor suppressor. *Cell Cycle*. 2011;10(19):3284-3299. doi:10.4161/cc.10.19.17176

42. Giovinazzo H, Walker D, Wyhs N, et al. A high-throughput screen of pharmacologically active compounds for inhibitors of UHRF1 reveals epigenetic activity of anthracycline derivative chemotherapeutic drugs. *Oncotarget*. 2019;10(32):3040-3050. doi:10.18632/oncotarget.26889

43. Singh AK, Yu X. Novel therapeutic targeting of UHRF1 restores 5′-azacytidine response in resistant acute myeloid leukemia. *Blood*. 2018;132(Suppl 1):1356-1356. doi:10.1182/blood-2018-99-115735

44. Senisterra G, Zhu HY, Luo X, et al. Discovery of small-molecule antagonists of the H3K9me3 binding to UHRF1 tandem Tudor domain. *SLAS Discov*. 2018;23(9):930-940. doi:10.1177/2472555218766278

45. Chang L, Campbell J, Raji IO, et al. Discovery of small molecules targeting the tandem Tudor domain of the epigenetic factor UHRF1 using fragment-based ligand discovery. *Sci Rep*. 2021;11:1121. doi:10.1038/s41598-020-80588-4

46. Houliston RS, Lemak A, Iqbal A, et al. Conformational dynamics of the TTD-PHD histone reader module of the UHRF1 epigenetic regulator reveals multiple histone-binding states, allosteric regulation, and druggability. *J Biol Chem*. 2017;292(51):20947-20959. doi:10.1074/jbc.M117.799700

47. Gelato KA, Tauber M, Ong MS, et al. Accessibility of different histone H3-binding domains of UHRF1 is allosterically regulated by phosphatidylinositol 5-phosphate. *Mol Cell*. 2014;54(6):905-919. doi:10.1016/j.molcel.2014.04.004

48. Brameier M, Krings A, MacCallum RM. NucPred—predicting nuclear localization of proteins. *Bioinformatics*. 2007;23(9):1159-1160. doi:10.1093/bioinformatics/btm066

49. Nguyen Ba AN, Pogoutse A, Provart N, Moses AM. NLStradamus: a simple hidden Markov model for nuclear localization signal prediction. *BMC Bioinformatics*. 2009;10(1):202. doi:10.1186/1471-2105-10-202

50. Lin J, Hu J. SeqNLS: Nuclear Localization Signal Prediction Based on Frequent Pattern Mining and Linear Motif Scoring. *PLoS ONE*. 2013;8(10):e76864. doi: 10.1371/journal.pone.0076864

51. Uversky VN. Intrinsically disordered proteins from a to Z. *Int J Biochem Cell Biol*. 2011;43(8):1090-1103. doi:10.1016/j.biocel.2011.04.001

52. Uversky VN, Gillespie JR, Fink AL. Why are "natively unfolded" proteins unstructured under physiologic conditions? *Proteins Struct Funct Bioinformatics*. 2000;41(3):415-427. doi:10.1002/1097-0134 (20001115)41:3<415::AID-PROT130>3.0.CO;2-7

53. Müller-Späth S, Soranno A, Hirschfeld V, et al. Charge interactions can dominate the dimensions of intrinsically disordered proteins. *PNAS*. 2010;107(33):14609-14614. doi:10.1073/pnas.1001743107

54. Wohl S, Jakubowski M, Zheng W. Salt-dependent conformational changes of intrinsically disordered proteins. *J Phys Chem Lett*. 2021;12(28):6684-6691. doi:10.1021/acs.jpclett.1c01607

55. Slabinski L, Jaroszewski L, Rychlewski L, Wilson IA, Lesley SA, Godzik A. XtalPred: a web server for prediction of protein crystallizability. *Bioinformatics*. 2007;23(24):3403-3405. doi:10.1093/bioinformatics/btm477

56. Ward JJ, McGuffin LJ, Bryson K, Buxton BF, Jones DT. The DISOPRED server for the prediction of protein disorder. *Bioinformatics*. 2004;20(13):2138-2139. doi:10.1093/bioinformatics/bth195

57. He B, Wang K, Liu Y, Xue B, Uversky VN, Dunker AK. Predicting intrinsic disorder in proteins: an overview. *Cell Res*. 2009;19(8):929-949. doi:10.1038/cr.2009.87

58. Tompa P, Schad E, Tantos A, Kalmar L. Intrinsically disordered proteins: emerging interaction specialists. *Curr Opin Struct Biol*. 2015;35:49-59. doi:10.1016/j.sbi.2015.08.009

59. Hansen JC, Lu X, Ross ED, Woody RW. Intrinsic protein disorder, amino acid composition, and histone terminal domains. *J Biol Chem*. 2006;281(4):1853-1856. doi:10.1074/jbc.R500022200

60. Darling AL, Uversky VN. Intrinsic disorder and posttranslational modifications: the darker side of the biological dark matter. *Front Genet*. 2018;9:158. doi:10.3389/fgene.2018.00158

SUPPORTING INFORMATION

Additional supporting information may be found in the online version of the article at the publisher's website.